

Sealing efficiency of cement-based materials containing extruded cementitious capsules

*Original*

Sealing efficiency of cement-based materials containing extruded cementitious capsules / Anglani, Giovanni; Van Mullem, Tim; Zhu, Xuejiao; Wang, Jianyun; Antonaci, Paola; De Belie, Nele; Tulliani, Jean-Marc; Van Tittelboom, Kim. - In: CONSTRUCTION AND BUILDING MATERIALS. - ISSN 0950-0618. - STAMPA. - 251:(2020), pp. 1-15. [10.1016/j.conbuildmat.2020.119039]

*Availability:*

This version is available at: 11583/2812332 since: 2025-02-18T08:15:35Z

*Publisher:*

Elsevier

*Published*

DOI:10.1016/j.conbuildmat.2020.119039

*Terms of use:*

This article is made available under terms and conditions as specified in the corresponding bibliographic description in the repository

*Publisher copyright*

Elsevier postprint/Author's Accepted Manuscript

© 2020. This manuscript version is made available under the CC-BY-NC-ND 4.0 license  
<http://creativecommons.org/licenses/by-nc-nd/4.0/>. The final authenticated version is available online at:  
<http://dx.doi.org/10.1016/j.conbuildmat.2020.119039>

(Article begins on next page)

# Sealing efficiency of cement-based materials containing extruded cementitious capsules

Giovanni Anglani<sup>a,\*</sup>, Tim Van Mullem<sup>b</sup>, Xuejiao Zhu<sup>b,c</sup>, Jianyun Wang<sup>d</sup>, Paola Antonaci<sup>a</sup>, Nele De Belie<sup>b</sup>, Jean-Marc Tulliani<sup>e</sup>, Kim Van Tittelboom<sup>b</sup>

<sup>a</sup>Department of Structural, Geotechnical and Building Engineering, Politecnico di Torino, Corso Duca degli Abruzzi 24, 10129 Torino, Italy

<sup>b</sup>Magnel-Vandepitte Laboratory for Structural Engineering and Building Materials, Faculty of Engineering and Architecture, Ghent University, Tech Lane Ghent Science Park, Campus A, Technologiepark Zwijnaarde 60, B-9052 Ghent, Belgium

<sup>c</sup>Center for Microbial Ecology and Technology, Department of Biotechnology, Faculty of Bioscience Engineering, Ghent University, Coupure Links 653, B-9000 Ghent, Belgium

<sup>d</sup>Department of Civil Engineering, Xi'an Jiaotong University, Yanxiang Road 99, 710054, Xi'an, China

<sup>e</sup>Department of Applied Science and Technology, Politecnico di Torino, Corso Duca degli Abruzzi 24, 10129 Torino, Italy

---

## Abstract

The intensive use of cement-based building materials is a growing concern in terms of environmental impact, since they significantly contribute to the global anthropogenic CO<sub>2</sub> emissions. The development of self-sealing cementitious materials could be a possible approach to improve the structural durability and thus reduce overall cost and environmental impact. In the present work, the efficiency of a self-sealing system using extruded cementitious capsules was experimentally investigated, and different healing agents were tested (specifically, a water-repellent agent, a polyurethane precursor and a solution of silica gel immobilized ureolytic bacteria). The self-sealing efficiency was evaluated in terms of capability to autonomously seal localized cracks induced in a controlled way. An active crack width control technique was adopted during the cracking procedure, in order to reduce the variation of the crack width within a series of specimens. Water permeability and capillary water absorption tests were performed to quantify the crack sealing ability, along with qualitative visual analysis of the crack faces. Positive results were achieved when using the water-repellent agent in water absorption tests, the bacterial agent in water-flow tests and the polyurethane precursor in both cases. This suggests that the proposed self-sealing system is sufficiently versatile to be used with different healing agents and that it can be effective in prolonging the material functionality by selecting the most appropriate agent for the real operating conditions.

*Keywords:* Self-sealing; Extruded cementitious capsules; Polyurethane; Water repellent agent; Bacteria; Durability; Water flow; Capillary water absorption

---

## 1. Introduction

Concrete is the most widely used building material on earth, with an estimated yearly consumption approaching 30 billion tons [1]. However, the cement manufacturing industry is currently under scrutiny because of the large volumes of CO<sub>2</sub> emitted during the production of Portland cement, since the production of cement contributes about 5-10% to

---

\* Corresponding author.

E-mail address: giovanni.anglani@polito.it (G. Anglani).

38 the global anthropogenic CO<sub>2</sub> emission, through the calcination process of limestone and  
39 combustion of fuels in the kiln [1,2]. In view of this problem, research in the construction  
40 and building materials sector is targeting alternative materials to partly or totally replace the  
41 ordinary Portland cement, such as supplementary cementitious materials derived from  
42 industrial by-products [3–6]. Moreover, the analysis of the carbon footprint of a structure  
43 also involves the estimation of its lifetime and the CO<sub>2</sub> emissions associated with its use,  
44 maintenance and repair. Indeed, the proper maintenance of a concrete structure and the  
45 selection of appropriate repair products and techniques is essential to guarantee and extend  
46 the designed lifetime [7], thus limiting the need for demolition and production of new  
47 concrete that would further increase the carbon footprint of the structure. Enhancing the  
48 longevity of the built environment will undoubtedly reduce the impact of human activities  
49 on the stability of the biosphere [8].

50 In the last decade, significant advancements have been achieved concerning the  
51 enhancement of the longevity of the built environment, by moving from passive repair  
52 approaches, that require an external manual intervention, to active methods that are  
53 incorporated at the construction stage and are regarded as self-sealing or self-healing  
54 techniques [9,10]. The first implies the filling and sealing of the crack, thus mitigating the  
55 ingress of deleterious substances present in the environment, the latter implies the recovery  
56 of the material properties as a consequence of the crack sealing [11,12]. Many different  
57 self-healing or self-sealing strategies for concrete have been developed and studied,  
58 comprising stimulated autogenous healing via use of mineral additives [13–16], crystalline  
59 admixtures [17–21] or superabsorbent polymers [22–27] and the autonomous healing  
60 mechanisms via use of micro-capsules [28–30], macro-capsules [31–38] or vascular  
61 systems [39–43], either using polymers [44–47], minerals [48–51] or bacteria [52–54] as  
62 healing agents. As regards the macro-encapsulation approaches, several types of capsules  
63 were thoroughly investigated by varying their shape, dimension and constituent material.  
64 Several requirements must be fulfilled in order to obtain effective systems: capsules should  
65 be compatible both with concrete and the encapsulated healing agent to protect it for a long  
66 time; they should be crack-responsive and able to release their content in order to fill and  
67 repair the cracks once formed, yet at the same time they should be able to resist the  
68 concrete mixing and casting processes. Finally, they should not affect the concrete  
69 mechanical properties significantly. In many studies, glass capsules were successfully used  
70 [32,35–38,55–59]. However, glass capsules may have a negative effect on concrete  
71 durability because of the possible onset of undesired alkali-silica reactions [9,34]. In  
72 addition, the likeliness that these stay intact during mixing is low unless proper additional  
73 precautions are taken [33,34,60–62]. In previous studies, the use of cementitious hollow  
74 tubes (CHTs) produced with an extrusion process [63–66] was proven effective in meeting  
75 the above mentioned requirements while presenting an inherent compatibility between the  
76 capsules shell and the cementitious matrix. In fact, although requiring additional  
77 waterproofing coating procedures with respect to the glass capsules, the cementitious tubes  
78 were able to protect and release effectively several types of healing agents (i.e. minerals  
79 and polymers), they showed a flexural strength comparable to that of cementitious mortar  
80 and they exhibited the ability to survive the mixing process. Moreover, they offered good  
81 performance recovery also in the presence of large cracks.

In this study, further modification to the tubular capsules' mix design, coating and sealing techniques were made in order to optimize the extrusion process and to improve the ability of the capsules to protect different types of healing agents, taking into consideration their various encapsulation requirements, including the possible need to encapsulate highly water-reactive substances. Specifically, it was decided to encapsulate one healing agent for each of the main groups of healing substances, based also on previous successful findings: a silane-based water repellent agent (WRA) [34] for the group of mineral substances, a one-component polyurethane (PU) precursor [59] for the group of polymeric substances and a ureolytic bacterial strain (i.e. *Bacillus sphaericus*) dispersed in silica sol (BS) and its deposition medium (DM) [38] for the group of biological substances. The efficiency of the system was assessed by evaluating the self-sealing of pre-cracked mortar specimens with embedded cementitious capsules. The sealing efficiency can be classified as recovery in durability-related properties, since durability can be increased when self-sealing of cracks results in retrieval of water tightness, thus preventing the penetration of aggressive liquids along these cracks into the matrix, which could cause further damage [10]. A cement mortar was used as a cementitious material prototype due to its homogeneity and ability for fast screening of the proposed self-sealing technology, before upscaling it for use in concrete [67]. The sealing efficiency was evaluated by means of water permeability and water absorption tests, in combination with the visual inspection of the cross sections after final rupture. A novel active crack control technique [67] was implemented in order to reduce the variability on the crack width obtained during the pre-cracking procedure and consequently the variability on the water permeability and absorption tests.

## 2. Materials

### 2.1. Healing agents

As mentioned in the previous section, three different healing agents were encapsulated. The first, denoted as WRA, is a commercially available water-repellent agent (Sikagard<sup>®</sup>-705 L, Sika, Switzerland). It is a 1-component silane-based and solvent-free reactive water repellent, with an approximate viscosity of 1.9 mPas at 25 °C. The product is commonly used in the construction sector as a water-repellent penetrating sealer for hydrophobic treatment of concrete and cementitious substrates. The WRA cures upon penetration in the substrates through chemical reactions that form covalent bonds with the minerals naturally present in the substrate.

The second healing agent, denoted as PU, is a commercially available polyurethane precursor (HA Flex SLV AF, De Neef Conchem, Belgium). It is a 1-component methylene diphenyl diisocyanate (MDI) and polyether-polyol-based prepolymer, which contains inert hydrophobic compounds that control the viscosity and rheological behavior, with an approximate viscosity of 200 mPas at 25 °C. The product is commonly used in the construction sector for grouting joints or stopping water leaks in concrete structures, which

120 are subject to settlement and movement, and for stopping water leaks through joints  
121 between tunnel segments. The PU precursor cures upon contact with moisture to a tough,  
122 flexible, closed-cell polyurethane foam.

123 The last healing agent consists of a ureolytic bacterial strain denoted as BS (*Bacillus*  
124 *sphaericus* LMG,22257, Belgian coordinated collection of microorganisms, Ghent),  
125 coupled with a suitable deposition medium, referred to as DM. In previous research, *B.*  
126 *sphaericus* was found to be able to precipitate calcium carbonate ( $\text{CaCO}_3$ ) on its cell  
127 constituents and in its micro-environment by decomposition of urea ( $\text{CO}(\text{NH}_2)_2$ ) into  
128 ammonium ( $\text{NH}_4^+$ ) and carbonate ( $\text{CO}_3^{2-}$ ) ions. The latter subsequently promotes the  
129 microbial deposition of  $\text{CaCO}_3$  in a calcium-rich environment. While the previous healing  
130 agents result in almost immediate crack sealing after release and curing, in this case the  
131 sealing needs some time and it is obtained through submersion in water, which will cause  
132 the activation of the bacteria and the subsequent precipitation of  $\text{CaCO}_3$ . This strain has a  
133 high urease activity (40 mM urea hydrolyzed.  $\text{OD}^{-1} \text{h}^{-1}$ ), long survival time and can produce  
134  $\text{CaCO}_3$  in a simple and controllable way [38]. Bacterial cells were used as a first proof of  
135 their compatibility with the extruded cementitious capsules, although it has to be remarked  
136 that the cells cannot remain viable for a long time inside the capsules and therefore spores  
137 (dormant bacteria) should be used to heal cracks appearing at a later age. The medium used  
138 to grow *B. sphaericus* consisted of yeast extract and urea. The yeast extract medium was  
139 first autoclaved for 20 min at 120 °C and the urea solution was added, which was sterilized  
140 by means of filtration through a sterile 0.22  $\mu\text{m}$  Millipore filter (Millipore, USA). The final  
141 concentrations of yeast extract and urea were 20 g/L. Cultures were incubated at 28 °C on a  
142 shaker at 100 rpm for 24 h. Bacterial cells were harvested by centrifuging (7000 rpm, 7  
143 min, Eppendorf MiniSpin, Hamburg, Germany) the 24 hours-old grown culture and the  
144 cells were resuspended in saline solution (NaCl, 8.5 g/L). The concentration of bacterial  
145 cells in the bacterial suspension (BS) was  $10^9$  cells/mL, determined by flowcytometry  
146 (Accuri C6, BD Biosciences, USA). In order to provide a suitable carrier to immobilize  
147 bacteria and to protect them from the harsh environment in concrete, before encapsulation,  
148 the BS was mixed (volume ratio 1:1) with a colloidal silica-sol (Levasil® CS30-316P,  
149 Obermeier, Germany) with a viscosity lower than 20 mPas at 20 °C. Additionally, a  
150 deposition medium (DM) consisting of 20 g/L urea and 79 g/L  $\text{Ca}(\text{NO}_3)_2 \cdot 4\text{H}_2\text{O}$  was  
151 provided separately, in order to allow the carbonate precipitation induced by the urease  
152 activity. The BS mixed with silica-sol and the DM were provided in separate capsules, as  
153 explained in the following Sections.

## 154 2.2. Extruded Cementitious Capsules

155 Cementitious tubular capsules were used as protecting and releasing carrier for the  
156 healing agents. They were produced in accordance with previous research [63,64], with  
157 some modification to the mix design of the cement paste and to the capsule coating and

sealing, aimed to improve the extrusion process and the protection/release behavior of the healing agents.

In order to reach a good workability and to avoid the collapse of the fresh extruded elements, several compounds were added to the cement paste [68,69]. The mix design included:

- Ordinary Portland cement (CEM I 52.5 R, Buzzi Unicem, Italy);
- Demineralized water;
- Copolymer of ethyl acrylate and MMA (Primal B60A, Sinopia s.a.s., Italy);
- Polyethylene glycol (PEG, Sigma Aldrich, Italy);
- Hydroxypropyl methylcellulose (HPMC, Sigma Aldrich, Italy);
- Calcium carbonate (CaCO<sub>3</sub>, Sinopia s.a.s., Italy);
- Metakaolin (halloysite from Applied Minerals Inc., USA, calcined at 650°C for 3 h)

First, all liquids were mixed together with an overhead stirrer (RW 20, Janke and Kunkel IKA, Germany); then, cement was added progressively, as well as the other powder compounds. Whenever necessary, to produce tubes free of defects, small quantities of cement, metakaolin and demineralized water were added during the extrusion procedure to adjust the workability of the paste, since the process is rather sensitive to the ambient temperature and relative humidity (RH). The mix design of the polymer-modified cement paste is detailed in Table 1.

**Table 1.** Mix design of the cement paste for the extrusion of the capsules' shell.

Water/cement ratio (-)	Cement (wt%)	Water (wt%)	Primal (wt%)	PEG (wt%)	HPMC (wt%)	CaCO <sub>3</sub> (wt%)	Metakaolin (wt%)
0.46	42.5	19.6	15.7	1.6	0.7	19.6	0.3

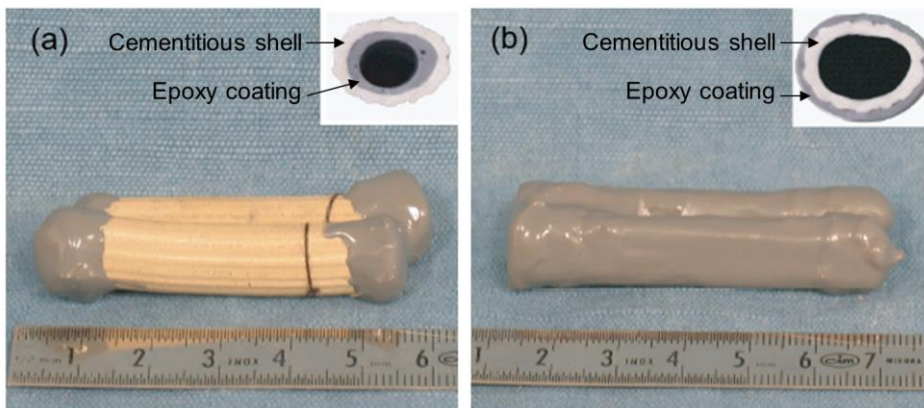
The fresh cement paste was extruded by using a low-pressure device composed of a screw extruder and replaceable dies [63,64]. The die had a ridged ring shape, with an external diameter of 10 mm and an internal diameter of 7.5 mm. After extrusion, the fresh cementitious elements, in the shape of hollow cylinders, were left in a moist environment (T≈20 °C, RH>95%) for 7 days and later in air (T≈20 °C, RH≈60%) for complete curing (t>28 days), as suggested in the literature for polymer-modified cementitious mortars [70]. The cylinders were further cut with a saw into tubes measuring about 5 cm in length.

In order to improve the conservation of the healing agents and the shock resistance of the capsules' shell, the tubes were further coated. First, a layer of a two-component epoxy primer (Primer AQ, API SpA, Italy) was applied by complete immersion of the tubes. Subsequently, a coating layer was applied by using a two-component epoxy resin (Plastigel, API SpA, Italy). This layer (thickness≈1 mm) was applied in two ways to the tubes, thus obtaining two types of capsules' shells presenting either an:

- 193 1. *Internal coating*: the epoxy resin was applied only to the internal surface by  
194 injection;
- 195 2. *External coating*: the epoxy resin was applied only to the exterior surface with a  
196 brush.

197 The application of an internal coating resulted in the reduction of the internal volume of  
198 the capsules, and hence in a reduction in the storable healing agent. Namely, the capsules  
199 with the external coating contained about 50% more healing agent with respect to the  
200 internally coated ones. However, it was chosen not to increase the length of the internally  
201 coated capsules in order not to increase their encumbrance and the capillary actions exerted  
202 during the agents' release, which were already higher due to the smaller internal radius.

203 Some tubes of both types were glued together with cyanoacrylate, in order to make them  
204 suitable to encapsulate two-component healing agents (i.e. the bacterial healing agent, see  
205 Section 2.1). Then, one end of the tube, either for single or coupled capsules, was sealed  
206 using an epoxy-based two-component thixotropic plaster (Stucco K, API SpA, Italy) and  
207 subsequent coating with Plastigel. At this stage, the healing agents were injected with a  
208 syringe until complete filling. Finally, the second end of the tube was sealed in the same  
209 way as the other, eventually generating a cementitious tubular capsule. Fig. 1 shows an  
210 example of the extruded capsules with their different types of coatings.



211  
212 **Fig. 1.** Extruded cementitious capsules with (a) internal and (b) external epoxy coating (outside view and  
213 cross section).

### 214 2.3. Mortar specimens

215 The self-sealing efficiency of the different healing agents encapsulated in the  
216 cementitious capsules was evaluated by using mortar specimens. The mortar was made with  
217 a water-to-cement ratio of 0.5 and a sand-to-cement ratio of 3, by using tap water,  
218 standardized sand (grading 0/2, DIN EN 196-1) and ordinary Portland cement (CEM I 52.5  
219 N, Holcim, Belgium). The mixing procedure was in accordance with EN 196-1. The fresh

conglomerate was used to fill prismatic molds covered with demolding oil (40 by 40 by 160 mm<sup>3</sup>), which contained the capsules and a smooth steel bar (diameter of 5 mm) also covered with demolding oil. The bar was positioned centrally, with its center at 12.5 mm from the top side of the specimen, and it was covered with demolding oil in order to ensure its easy removal after casting, in such a way to create a longitudinal hole in the specimen. The capsules were placed at 7.5 mm from the bottom side of the specimens by gluing them on two thin nylon threads connected to the lateral side of the molds, to fix their position (Fig. 2).



**Fig. 2.** Cementitious capsule fixed at its position at the bottom of the molds with nylon threads before the positioning of the oiled bar and casting (cross section in Fig. 3).

After the specimens were cast, they were covered with plastic foil and stored in an air-conditioned room at a temperature of  $(20 \pm 2)$  °C. The day after casting, the steel bar was removed from the specimens when they were demolded. The specimens were then wrapped again in plastic foil and stored at  $(20 \pm 2)$  °C until the age of 7 days.

Four different series were made: two series containing a single capsule filled with the water-repellent agent (WRA series) or the PU precursor (PUR series); one series containing two coupled capsules, one filled with the bacterial suspension and silica-sol mix and the other capsule filled with the deposition medium as mentioned in Section 2.1 and Section 2.2 (BAC series); one final series consisting of reference specimens without capsules/healing agent (REF series). Each series containing capsules consisted of 8 specimens, 4 of which had capsules with external coating and 4 with internal coating (see Section 2.2, Figure 1), while the REF series consisted of 6 specimens. Table 2 summarizes the test series, while Fig. 3 shows the schematic cross section of all the prepared specimens.

**Table 2.** Test series used to evaluate the self-sealing efficiency.

Series	Healing agent	Number of capsules per specimen	Capsule coating	Number of specimens
--------	---------------	---------------------------------	-----------------	---------------------



REF	None	None	-	6
WRA	Water-repellent agent	One capsule	Internal	4
			External	4
PUR	Polyurethane precursor	One capsule	Internal	4
			External	4
BAC	<i>B. Sphaericus</i> mixed with silica-sol + Deposition Medium	Two coupled capsules	Internal	4
			External	4

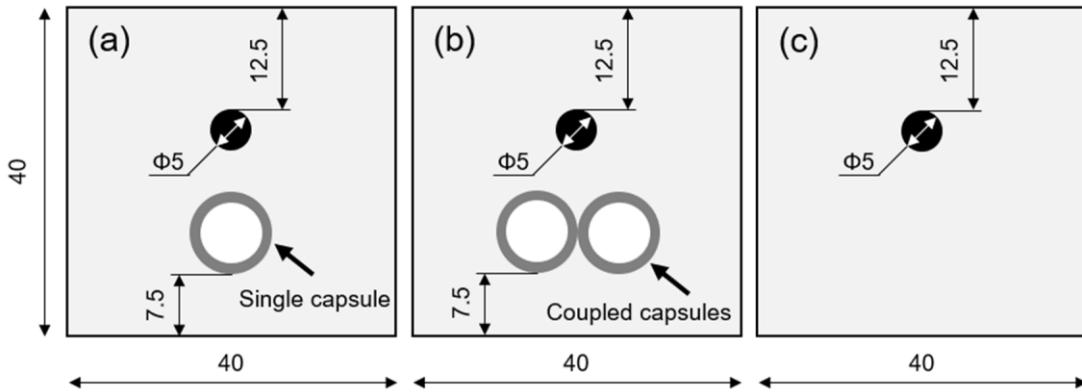


**Fig. 3.** Schematic cross section of the specimen containing either (a) one capsule (WRA and PUR series), (b) two coupled capsules (BAC series) or (c) no capsules (REF series). Dimensions expressed in mm.

### 3. Methods

#### 3.1. Crack creation and crack width control technique

In order to evaluate the sealing efficiency of the proposed system, a preliminary cracking has first to be induced in the specimens [12]. In the attempt to reduce the variability of the crack widths produced by pre-cracking in 3-point bending, and consequently the variability on the sealing results, a novel active crack width control technique was adopted [67]. A Carbon Fiber Reinforced Polymer (CFRP) strip (PC<sup>®</sup> CARBOCOMP UNI, TRADECC, Belgium) with dimensions of 40 mm by 160 mm was glued on the top side of the mortar specimens a day before pre-cracking by using an epoxy adhesive (Sikadur<sup>®</sup>-30, Sika, Switzerland). The CFRP strip consisted of unidirectional carbon fibers embedded in epoxy resin. At the age of 7 days from casting, the specimens were cracked until failure in a 3-point bending test setup with a span of 10 cm and at a load rate of 50 N/s. Due to the presence of the CFRP strip, both halves of the mortar specimens divided by the through-going crack created via the 3-point bending test remained connected on top by the laminate, presenting however a large crack between them. As a result of the stiffness of the CFRP, the two halves could only move with one degree of freedom, that was the rotation around the line on top of the through-going crack connected by the laminate. Hence, the crack

could be narrowed but the two halves could not rotate relative to each other around their longitudinal axis. Immediately after cracking, the specimens were placed with their crack face upwards and the crack width was restrained using screw jacks using an iterative procedure of measuring and restraining until a desired crack width of 300  $\mu\text{m}$ . The crack width was determined using an optical stereo microscope (Leica S8APO mounted with a DFC295 camera). Along the length of the crack 3 locations were chosen randomly. For each location the crack width was determined by 4 to 5 measurements. The reported crack width  $w$  ( $\mu\text{m}$ ) is the average of all the measurements of the three locations (in total 12-15 measurements). Fig. 4 shows a specimen restrained with the active crack control technique.



**Fig. 4.** Typical sample for which the crack width was controlled using the active crack width control technique. In the figure it is possible to see the healing agent released from the ruptured capsule and spread around the crack mouth (dark colored zone)

Minimally 3 hours after crack creation, the cracks at the sides of the specimens were sealed with a methyl methacrylate glue (Schnellklebstoff X60, HBM, Germany) in order to subsequently perform the water flow and capillary water absorption tests (see Section 3.3). Specimens were then placed for one day in a curing room (at  $20 \pm 2$  °C, >95% RH) so as not to affect the curing of the healing agents in the first 24 h; subsequently they were immersed in demineralized water for 6 days. The one-day storage at  $20 \pm 2$  °C and >95% RH was done in order to avoid either washing away the uncured water-repelling agent (WRA series) or, on the contrary, facilitating the reaction of the unpolymerized polyurethane (PUR series) upon continuous contact with water, which could result in an additional filling of the crack. The specimens of the BAC series were directly immersed in demineralized water 5 hours after crack creation for 7 days.

### 3.2. Visual examination of the healing agents in the crack

After the crack creation and at different times after curing and testing, pictures of the crack mouths were taken using the optical stereo microscope. After completion of the sealing efficiency testing (see Sections 3.3 and 3.4), the samples were split at the location of the crack in order to evaluate the healing agent coverage on the crack faces [36,37,64].

296 This visual evaluation allowed to gain qualitative information on the ability of the healing  
297 agents to fill the cracks. In order to quantitatively determine the surface area of the spread  
298 region of the healing agents inside the crack, the crack faces of each sample were placed  
299 next to each other and a picture of the total crack surface was taken. For each of the crack  
300 faces, the area covered by the healing agent was determined using the photo editing  
301 software GIMP. The ratio between the crack faces covered by the healing agent and the  
302 total crack faces area was then denoted as the surface coverage of the crack faces.

### 303 *3.3. Water flow test*

304 Before crack creation, one side of the specimens was provided with a plastic tube (with  
305 external diameter of 6 mm) in order to connect the specimen to the water flow setup. In  
306 order to do this, the diameter of the cast-in hole was enlarged over a length of  $(25\pm 5)$  mm  
307 using a drill. The tube was inserted in the hole and a watertight connection was ensured by  
308 using silicone. At the other side of the specimens, the cast-in hole was sealed using the  
309 same silicone. Seven days after crack creation, the sealing efficiency of the self-sealing  
310 mortar was first assessed by measuring the water flow passing through the specimen, using  
311 a test procedure developed in the European project HEALCON [12,24,71]. The test  
312 requires the use of specimens which have to be saturated for at least 2 days by water  
313 submersion, in order to remove as much air bubbles out of the crack as possible and to  
314 prevent water absorption through the pores of the mortar matrix during testing. This  
315 requirement was fulfilled due to the curing of the specimens in demineralized water for 6 or  
316 7 days after crack creation. One side of the specimen was connected with a plastic tube to a  
317 water reservoir at a height of 500 mm with respect to the cast-in hole, while the other side  
318 of the specimen was completely sealed with silicone and the crack was sealed at the side  
319 surfaces with methyl methacrylate glue (Schnellklebstoff X60, HBM, Germany) after crack  
320 creation, so that the water could only leak out from the bottom of the crack (see Fig. 5).

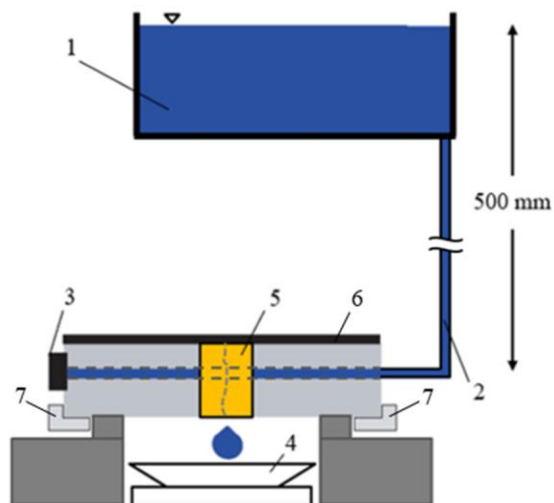


**Fig. 5.** Test setup for the water flow test: (1) water reservoir, (2) plastic tube, (3) silicone sealing, (4) scale, (5) sealing with methyl methacrylate glue, (6) CFRP strip, (7) screw jacks.

The water flow test was carried out one time on each specimen at a temperature of  $(20 \pm 2)$  °C and a relative humidity of  $(60 \pm 5)\%$ . The amount of leaked water was recorded over time for a minimum of 5 minutes on a scale with an automated registration system. However, the first 30 s of testing were not recorded to ensure that the error induced by the initial presence of air bubbles was removed by the flow of water through the crack and only a stable fully developed flow (i.e. linearly dependent on time) was studied. Out of this data, the flow rate  $q$  (g/min) was calculated. The sealing efficiency of a certain type of self-sealing specimens, containing the extruded cementitious capsules, was calculated with respect to the reference specimens, without capsules, using Equation 1:

$$SE_{wf}(\%) = \frac{q_{REF} - q_i}{q_{REF}} \times 100 \quad (1)$$

where  $SE_{wf}$  is the sealing efficiency assessed through the water flow test,  $q_{REF}$  the average water flow rate (g/min) of the reference specimens (REF, 6 specimens) and  $q_i$  the average water flow rate (g/min) of the self-sealing specimens containing capsules (4 specimens per series, distinguished according to the different healing agent used (WRA, PUR or BAC) and capsule coating (INT or EXT)).

### 3.4. Water absorption test

Measuring the capillary water absorption for cracked specimens with and without sealing can also be used to evaluate the crack sealing efficiency [11,35,36,64]. To this aim, the specimens previously used for the water flow test were first placed in an oven at 40 °C to

remove moisture (6 reference specimens, 4 specimens for the different self-sealing series distinguished according to the different healing agent used and capsule coating). Specimens were dried until constant mass (mass change less than 0.1% in 24 h) was achieved. After the drying period, the specimens were stored at  $(20 \pm 2) ^\circ\text{C}$  and  $(60 \pm 5)\%$  RH for 24 h. Then, the screw jacks used for the active crack width control technique (Section 3.1) were removed. The removal did not significantly affect the crack width and was done in order to cover the sides of the specimens over a height of 15 mm with a self-adhesive aluminum-butyl tape so that the water could only enter the samples through a predefined test surface around the crack. The bottom surface was also covered with the aluminum-butyl tape so that only a 20 mm wide zone around the crack was exposed to water during the absorption test (Fig. 6). The specimens were weighed and then placed on two rigid non-porous supports in a container with demineralized water and with only the lower 5 mm of the specimens immersed in water. After the start of the water absorption test, the specimens were all removed at the same time and then weighed at 5 min interval for the first half an hour, then at 30 min intervals until 4 h and every hour until 8 h, following the removal of the excess of water on their faces with absorbing paper. Time correction due to the removal was taken into account, stopping the time at each removal for the duration of the weighing procedures.

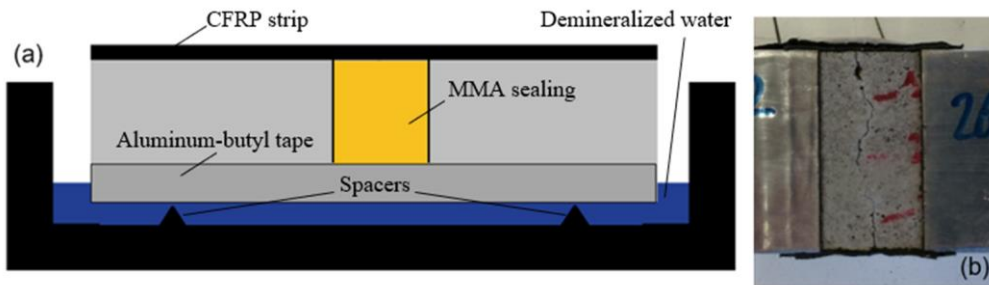


**Fig. 6.** Test setup for the water absorption test: (a) schematic illustration; (b) surface exposed to water ( $20 \times 40 \text{ mm}^2$ )

The test was carried out at a temperature of  $(20 \pm 2) ^\circ\text{C}$  and a relative humidity of  $(60 \pm 5)\%$ . The cumulative absorbed volume of water per unit area  $i$  ( $\text{mm}^3/\text{mm}^2$ ), defined as the change in mass (mg) divided by the density of water at the recorded temperature ( $\text{mg}/\text{mm}^3$ ) and by the water exposed area of the specimen ( $\text{mm}^2$ ), is generally plotted against the square root of time. The slope of the obtained line gives the sorptivity index  $S$  ( $\text{mm}/\text{s}^{0.5}$ ) of the specimen. However, recent studies questioned the calculation of the sorptivity index of cementitious materials by using the square root of time  $t$  (seconds), highlighting the lack of linearity that is often found using it [72]. The use of the fourth root of time was then demonstrated to be more effective in showing a linear evolution in the water uptake of non-cracked mortars due to the hygroscopicity of cementitious materials and swelling caused by the interaction with water (Eq. 2). This model was adopted also in this study.

$$i = S * t^{0.25} \quad (2)$$

The sealing efficiency of the self-sealing specimens, containing the extruded cementitious capsules, was calculated as a reduction of sorptivity with respect to the cracked reference specimens, without capsules, using Equation 3:

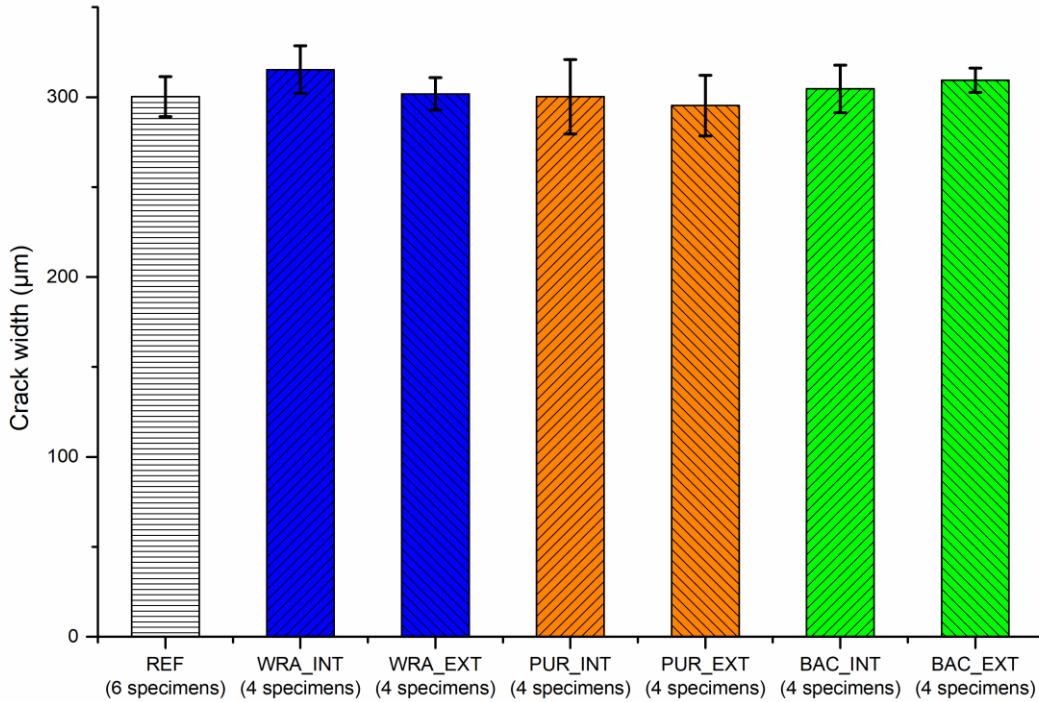
$$SE_{wa}(\%) = \frac{S_{REF} - S_i}{S_{REF}} \times 100 \quad (3)$$

where  $SE_{wa}$  is the sealing efficiency assessed through the water absorption test,  $S_{REF}$  the average sorptivity index ( $\text{mm}/\text{s}^{0.25}$ ) of the reference specimens (REF, 6 specimens) and  $S_i$  the sorptivity index ( $\text{mm}/\text{s}^{0.25}$ ) of the self-sealing specimens containing capsules (4 specimens per series, distinguished according to the different healing agent used (WRA, PUR or BAC) and capsule coating (INT or EXT)).

## 4. Results and discussion

### 4.1. Crack creation and crack width control technique

Fig. 7 shows the average crack width  $w$  ( $\mu\text{m}$ ) and the related standard deviation bars measured for the different series, distinguished according to the different healing agent used (REF, WRA, PUR and BAC) and the capsule coating (INT or EXT).



390

391  
392

**Fig. 7.** Average crack width  $w$  of each series after the active crack width control (error bars refer to  $\pm$  one standard deviation)

393

394

395

396

397

398

399

400

401

402

403

An analysis of variance (ANOVA) test was applied and it showed that the mean crack widths of the different test series were not significantly different from each other (level of significance=0.05,  $p=0.45$ ), making them comparable in terms of crack width.

Table 3 summarizes the average crack width  $w$ , the standard deviation  $\sigma_w$  and the resulting coefficient of variation  $CV$  of each series after the active crack width control. The highlighted variations are quite small if compared with the literature where other crack control techniques were used. For instance, coefficients of variation ranging from 6% to 20% were obtained for cylinders cracked through their depth and tied back together with spacers [73], while ranges of variation up to 40  $\mu\text{m}$  on the average crack width were measured on prismatic specimens cracked by using a crack-width controlled 3-point bending test [24].

404

405

**Table 3.** Overview of average crack width  $w$ , standard deviation  $\sigma_w$  and coefficient of variation  $CV$  of each series after the active crack width control.

Series	Coating	$w$ ( $\mu\text{m}$ )	$\sigma_w$ ( $\mu\text{m}$ )	$CV$ (-)
--------	---------	--------------------------	---------------------------------	-------------

REF	-	300	11	4%
WRA	INT	315	13	4%
	EXT	302	9	3%
PUR	INT	300	21	7%
	EXT	295	17	6%
BAC	INT	305	13	4%
	EXT	309	7	2%

406

407

408

409

410

411

412

These findings indicate that the active crack control technique can effectively reduce the variability of the crack width, which is a very important parameter when specimens should be subjected to permeability tests. Indeed, Edvardsen [74] stated that the permeability of a crack is related to the third power of the crack width. Nevertheless, it should be noted that permeability and absorption are strongly affected also by the internal geometry of the crack, on which no control can be exerted [12,67].

413

#### *4.2. Visual examination of the healing agents in the crack*

414

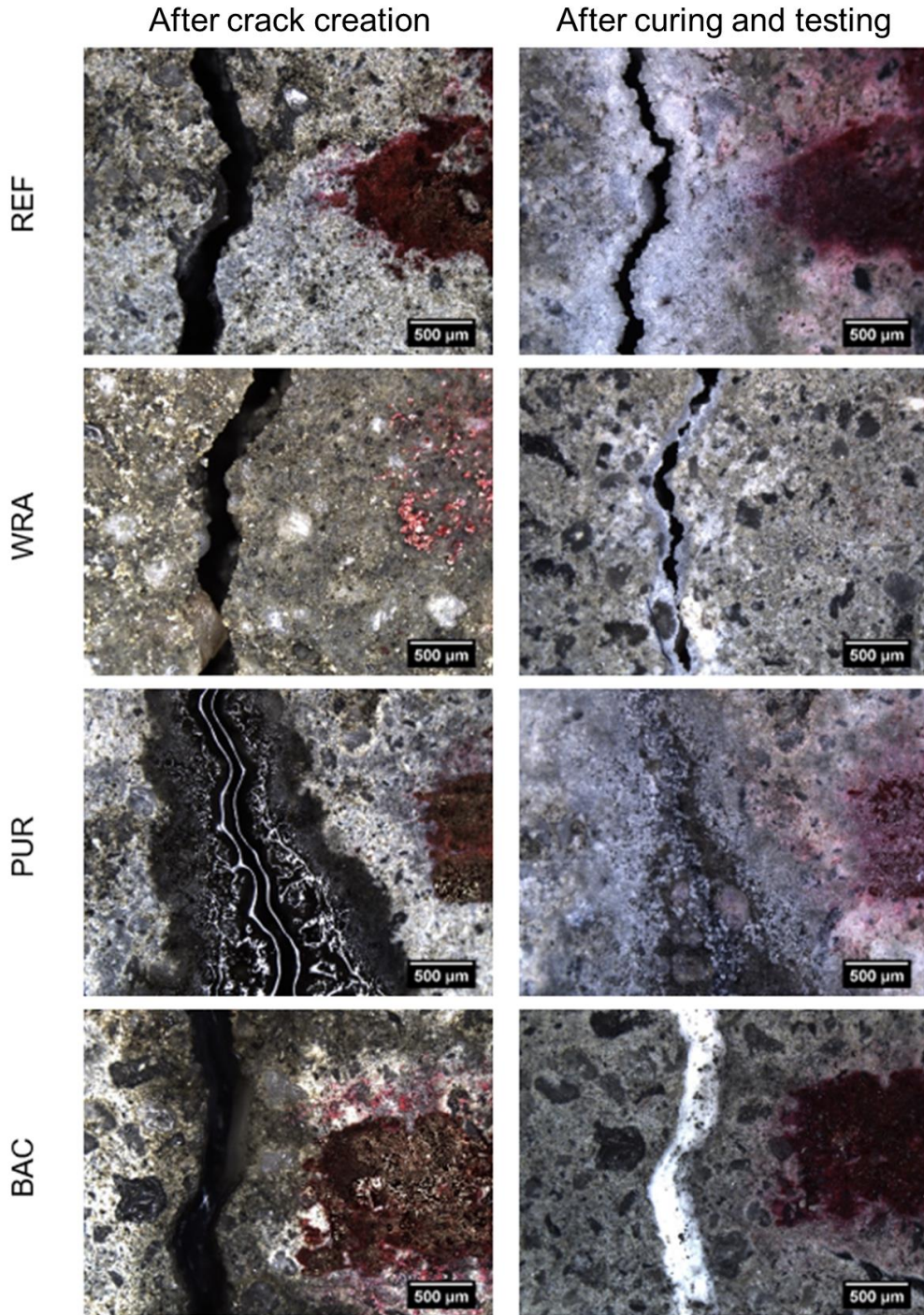
415

416

417

After the crack creation and at different times after curing and testing, pictures of the crack mouth were taken using an optical stereo microscope. Fig. 8 shows a comparison between the crack mouth at one fixed location for each series, immediately after crack creation and after curing and testing.





418

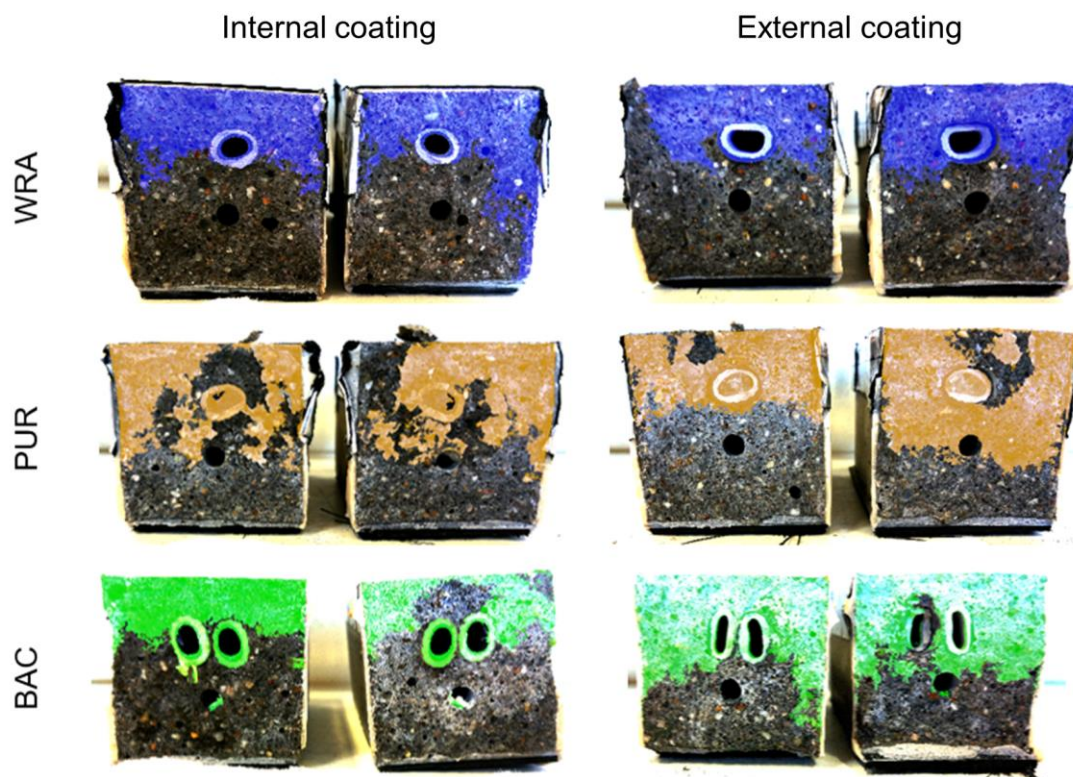
419

420

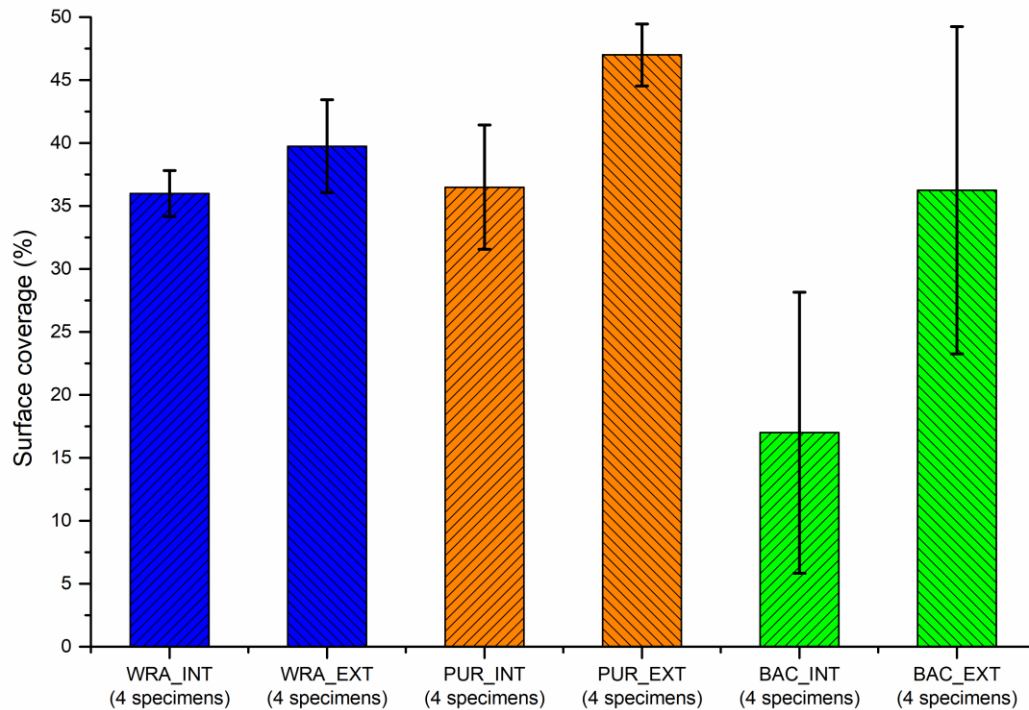
**Fig. 8.** Visualization of the crack mouths filled with the different healing agents, after crack creation, and after curing and testing, for some of the best cases observed.

421 It should be noted that also for the REF series, a crack sealing due to autogenous healing  
 422 was identifiable at the crack mouth. The WRA was mainly absorbed by the matrix due to its  
 423 low viscosity and was not able to grant a real crack filling, leaving the crack mouth opened.  
 424 On the contrary, the PU and the silica gel with the subsequent precipitation of  $\text{CaCO}_3$   
 425 provided a good crack filling, creating a barrier of healing agent that sealed the crack along  
 426 its length, in some case completely.

427 To complement the information gained from the micrographs of the crack mouth, the  
 428 specimens were split at the location of the crack, after performing the test described in  
 429 Section 3.3 and Section 3.4. The crack faces were then placed next to each other and a  
 430 picture of the crack faces was taken. The total area covered by the healing agents was  
 431 determined using a photo editing software. The ratio between the area of the crack faces  
 432 covered by the healing agents and the total area was then denoted as the surface coverage of  
 433 the crack faces, so to determine the spreading region of the healing agents inside the crack.  
 434 The area of the capsules was taken into account for the calculation of the total area of the  
 435 crack faces. Fig. 9 shows some representative crack faces and spread regions for each series  
 436 containing capsules, while Fig. 10 shows the average surface coverage (%).



437  
 438 **Fig. 9.** Visualization of the spreading region of the healing agents in the crack for mortar prisms containing  
 439 capsules with internal or external coating.



440

441  
442

**Fig. 10.** Average surface coverage of the healing agent on the crack faces for each series containing capsules (error bars refer to  $\pm$  one standard deviation)

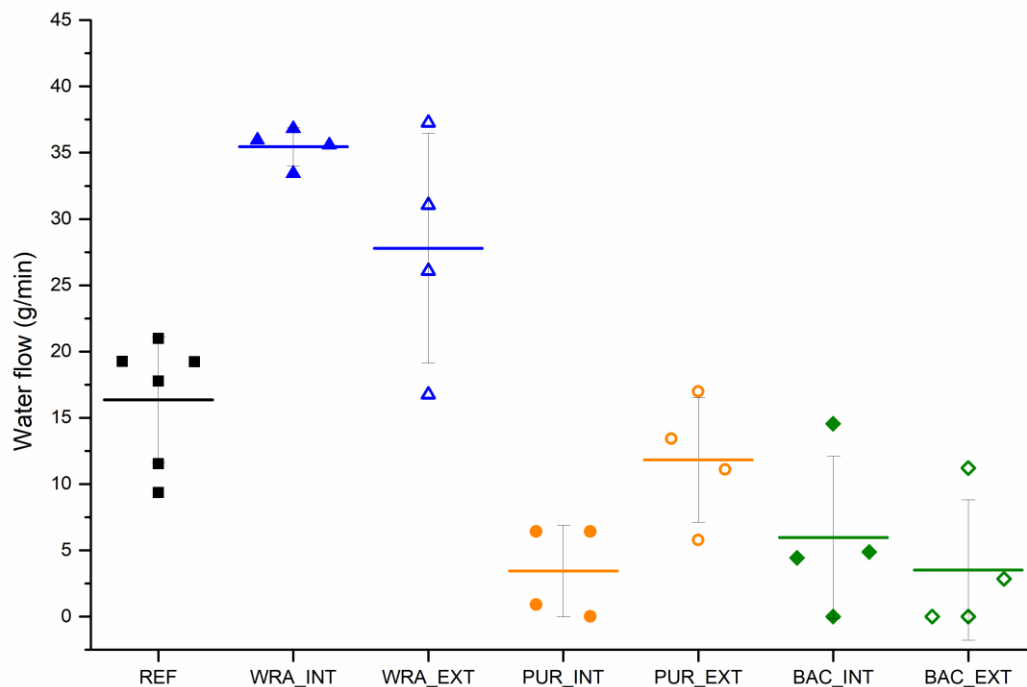
443  
444  
445  
446  
447  
448  
449  
450  
451  
452  
453  
454  
455  
456  
457

As it can be expected and preferred for sealing purposes, the portion of the crack faces that was mainly covered by the healing agents was the bottom part, above the crack mouth. In general, for a given healing agent, a slightly higher surface coverage was detected in the case of the specimens containing the capsules with the external coating, most likely due to the higher amount of healing agent carried by these capsules (see Section 2.2). Best spread over the crack faces was obtained when the PU precursor was used. Crack filling was also noticeable due to the presence of a thick PU foam over the crack faces. Moreover, the PU was able in most of the cases to seal also the cavity left by the capsules. The WRA series also showed a good spread over the crack faces, even if part of the water-repellent agent was lost during the pre-cracking procedure due to the very low viscosity of the healing agent. It is most likely that a large part of the WRA was absorbed by the mortar substrate at the crack faces due to its low viscosity, resulting in a hydrophobation of the crack faces rather than an actual crack filling, as already mentioned. In fact, it should be pointed out that the WRA was commercially designed to work as a cementitious substrate sealer by being absorbed in the superficial part of the matrix. The results of the BAC series showed a

458 higher dispersion. This can be ascribed to the fact that the BAC series is based on a two-  
 459 component healing agent. Hence, while in some cases an even distribution of the silica gel  
 460 that immobilized the bacteria was recognizable, in other cases there was a clear separation  
 461 of the portion covered by the gel and the portion covered by the deposition medium. Just  
 462 the surface portion that presented the silica gel was taken in consideration for assessing the  
 463 surface coverage. Last, it is to be underlined that, even though the BAC series with the  
 464 capsules with an internal coating were those with the smaller surface coverage, the  
 465 spreading area consisted of a thick white gel that filled the zone adjacent to the crack mouth  
 466 along its length.

#### 467 4.3. Water flow test

468 After curing in demineralized water for 7 days, the pre-cracked specimens were  
 469 subjected to the water flow test, as reported in Section 3.3. Fig. 11 shows the flow rate  $q$   
 470 (g/min) measured for the different series, distinguished according to the different healing  
 471 agent used (REF, WRA, PUR and BAC) and the capsule coating (INT or EXT).



472

473 **Fig. 11.** Water flow rate  $q$  of each series: individual samples results (symbols) and mean value of the series  
 474 (solid line, error is  $\pm$  one standard deviation)

475 An analysis of variance (ANOVA) test was applied and it showed that the mean values  
476 of the water flows of the different test series were significantly different from each other  
477 (level of significance=0.05,  $p=1.52 \cdot 10^{-8}$ ). After normality was assumed by means of a  
478 Shapiro-Wilk test ( $p=0.977$ ) and homogeneity of variance was assumed by means of a  
479 Levene's test (level of significance=0.01,  $p=0.26$ ), a Tukey test (level of significance=0.05)  
480 was used as post-hoc test in order to highlight which series were statistically different or  
481 equal in terms of water flow. When comparing two series with the same healing agent but  
482 different coating, the difference of their means was never significant at the 0.05 level of  
483 significance. Moreover, the test highlighted that the REF and WRA series (either with  
484 internal or external coating), being the series with the worst results in terms of water flow  
485 (high flow rate), were not significantly different from each other. Similarly, the PUR and  
486 BAC series (either with internal or external coating), being the series with the best results  
487 (low flow rate), turned out to be statistically undistinguishable. In fact, some specimens  
488 from these two series showed outstanding results, since absent or negligible water flow was  
489 detected, consequently presenting a 100% sealing efficiency  $SE_{wf}$  (Eq. 1), compared to the  
490 average flow rate of the REF series. Namely, 3 specimens from the BAC series showed a  
491 100% sealing efficiency (1 with internal and 2 with external coating), while for the PUR  
492 series one specimen showed a 100% and one specimen a 95% sealing efficiency (both with  
493 internal coating).

494 On the contrary, as mentioned above, poor results in terms of water flow (high flow rate)  
495 were obtained when the water-repellent agent was used. In fact, the use of this healing  
496 agent showed even detrimental effects on the performance of the series, with an average  
497 flow rate higher than that of the REF series. As already stated in Section 4.2, the WRA was  
498 most likely able to spread over the crack faces rather than fill the crack. In addition, for the  
499 WRA series the capsules were empty after releasing the low viscosity water repellent agent,  
500 contrary to what happened for the PUR series where also the cavities created by the  
501 capsules were sealed. The result was just the hydrophobation of the crack faces due to the  
502 curing mechanism of the WRA described in Section 2.1.

503 The effect of such hydrophobation is essentially to prevent the water absorption at low  
504 pressure, rather than stop a pressurized water leakage, as in the case of the water flow test.  
505 Hence, the water could leak downwards through the open crack during the water flow test  
506 without a substantial impediment.

507 This could have led to a further issue: it shall be considered that the specimens were pre-  
508 cracked at an early age (i.e. 7 days), when the autogenous healing mechanism is most  
509 relevant due to the presence of unhydrated binder particles and to the ongoing development  
510 of new CSH gels [9,74–78]. Water is an essential factor for autogenous healing and the  
511 water immersion has been reported as the best exposure for this type of self-sealing effect.  
512 Thus, by reducing the water absorption on the crack faces, the WRA could have reduced  
513 the continued hydration of unhydrated cement grains, hence the autogenous self-sealing,

514 that might have been higher in the REF series, as it is suggested by Fig. 8 comparing the  
 515 microscopic images of the crack mouths of these two series immediately after healing.

516 Table 4 summarizes the results of the water flow test, showing the best recovery for the  
 517 series that used the PU as healing agent and the internal coating of the capsules ( $SE_{wf}=79\%$ )  
 518 and the BAC series with external coating ( $SE_{wf}=78\%$ ).

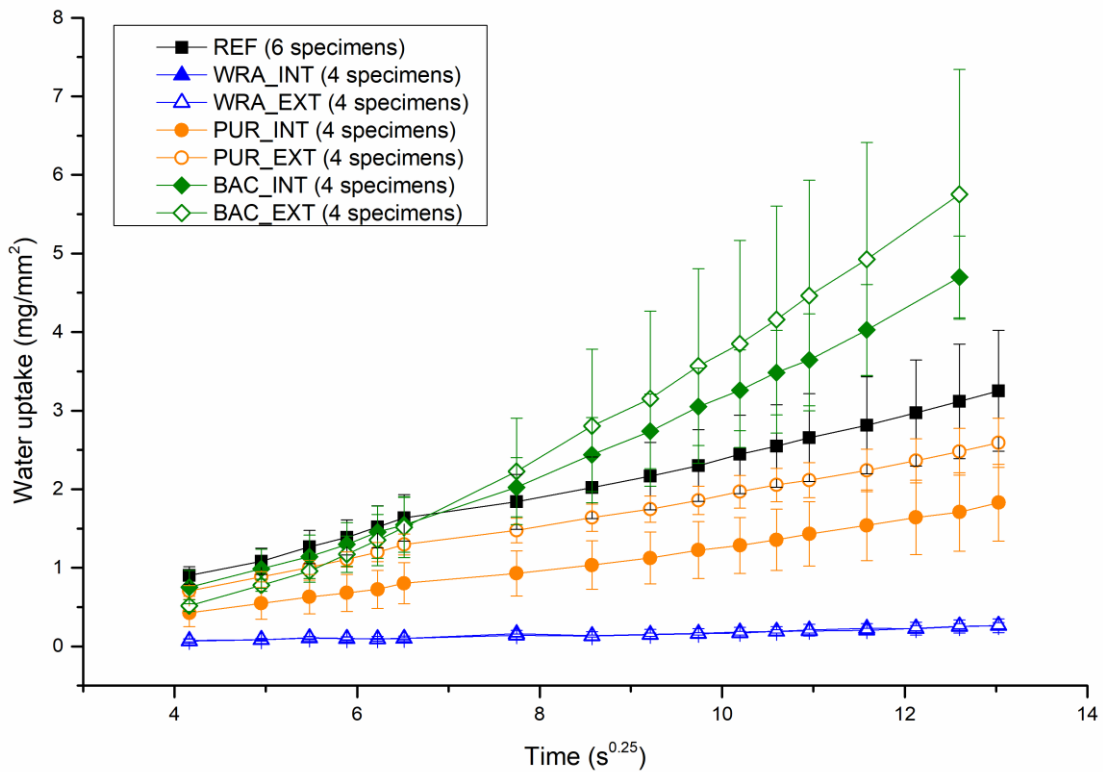
519 **Table 4.** Overview of average water flow rate  $q$ , standard deviation  $\sigma_q$  and average sealing efficiency  $SE_{wf}$  of  
 520 each series after the water flow test.

Series	Coating	$q$ (g/min)	$\sigma_q$ (g/min)	$SE_{wf}$ (-)
REF	-	16	5	-
WRA	INT	35	1	-117%
	EXT	28	9	-70%
PUR	INT	3	3	79%
	EXT	12	5	28%
BAC	INT	6	6	64%
	EXT	4	5	78%

521

#### 522 4.4. Water absorption test

523 After complete oven drying ( $T=40\text{ }^{\circ}\text{C}$ ), the specimens were subjected to a water  
 524 absorption test, as reported in Section 3.4. Fig. 12 shows the weight gained due to water  
 525 uptake plotted versus the fourth root of time for each series.

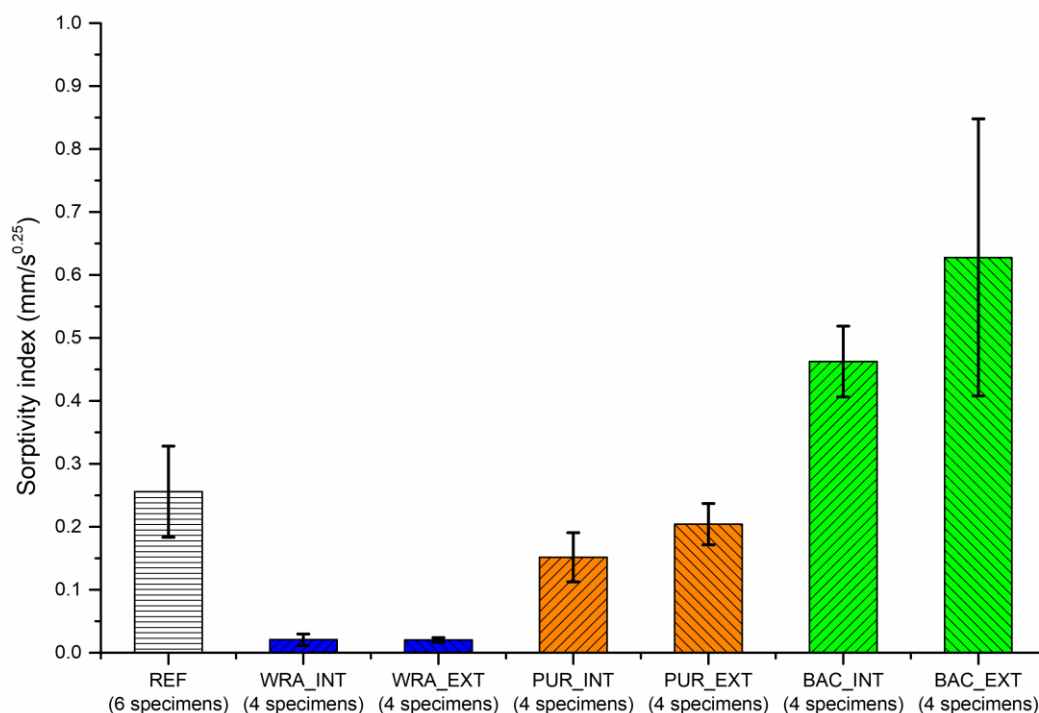


526

527 **Fig. 12.** Average water uptake of each series plotted versus the fourth square of time (error bars refer  $\pm$  one  
 528 standard deviation).

529 For each series, the coefficients of determination  $R^2$  by using linear regression were  
 530 respectively 0.9963, 0.9564, 0.9449, 0.9943, 0.9978, 0.9901 and 0.9904, showing that the  
 531 linear regression fits the data very well. It is possible to notice that the WRA series with  
 532 internal and external coating showed an almost identical behavior, characterized by a low  
 533 water uptake and a small scattering between different specimens.

534 The sorptivity index  $S$  ( $\text{mm}/\text{s}^{0.25}$ ) was calculated using Eq. 2, considering the cumulative  
 535 absorbed volume of water per unit area  $i$  ( $\text{mm}^3/\text{mm}^2$ ) between 5 minutes and 8 hours of  
 536 water absorption. Fig. 13 shows the  $S$  values measured for the different series, distinguished  
 537 according to the different healing agent used (REF, WRA, PUR and BAC) and the capsule  
 538 coating (INT or EXT).



539

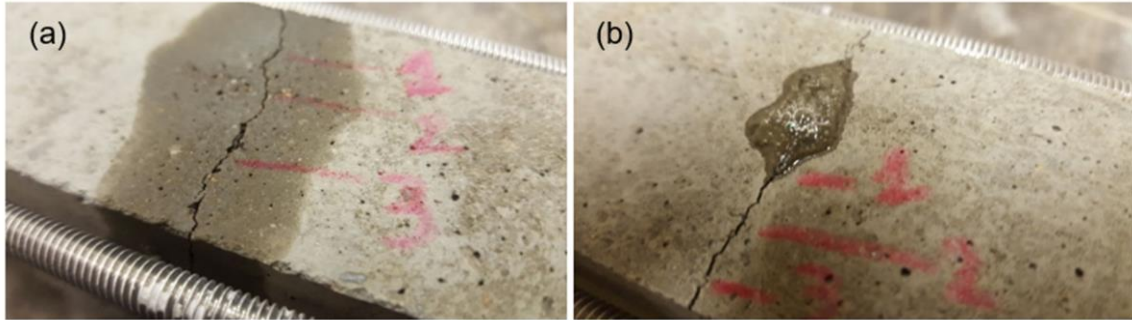
540 **Fig. 13.** Mean sorptivity index  $S$  of each series (error is  $\pm$  one standard deviation).

541 From the moment that it was not possible to assume normality by means of a Shapiro-  
 542 Wilk test ( $p=0.977$ ), a One Way ANOVA on Ranks by means of a Kruskal-Wallis test was  
 543 applied and it showed that there was a statistically significant difference between the  
 544 different test series medians ( $p<0.001$ ). A Dunn's test (level of significance= $0.05$ ) was used  
 545 as a post-hoc test in order to highlight which series were statistically different or equal in  
 546 terms of sorptivity. Again, when comparing two series with the same healing agent but  
 547 different coating, the difference was never significant at the  $0.05$  level of significance.

548 Positive results were obtained using the PU and the WRA. The WRA showed  
 549 outstanding results, contrary to those obtained during the water flow test (Section 4.3).  
 550 Indeed, a very slow absorption rate was detected, with almost perfect repeatability on each  
 551 specimen of the series. This excellent performance can be explained by the water-repellent  
 552 agent characteristics, since it is designed exactly with the aim of reducing the water  
 553 absorption of cementitious substrates. Moreover, during the pre-cracking procedure, the  
 554 WRA was spread both on the crack faces, thus penetrating in the mortar matrix, and also on  
 555 the area adjacent to the crack mouth, which was the area in contact with water during the  
 556 test (Fig. 14). This allowed to obtain an almost perfect protection against the water



557 absorption. The PUR series showed good results because of the good filling of the crack  
558 offered by the closed cell PU foam. However, a larger contribution of the matrix absorption  
559 rate can reasonably be considered for this series, because the healing agents did not cover  
560 the complete area adjacent to the crack as in the previous case (Fig. 14).



561

562 **Fig. 14.** Spread of the healing agent on the area adjacent to the crack mouth for (a) WRA and (b) PUR series  
563 after crack creation. The water-repellent agent covered the complete area in contact with water during the  
564 water absorption test.

565 On the other hand, poor results were obtained for the BAC series. In fact, the use of this  
566 healing agent showed even detrimental effects on the performance of the series, with a  
567 sorptivity index more than double of that of the REF series. This behavior could be  
568 attributed to several causes. The first cause could be ascribed to an intrinsic drawback of  
569 the water absorption used on self-sealing systems that is often debated. For instance, a  
570 partially healed crack could have a smaller crack width and thus a higher capillary force,  
571 resulting in a possible larger amount of water uptake compared to an unhealed crack  
572 [12,67]. This could be the case for the BAC series, were the partially closed crack could  
573 promote higher capillary forces if compared with the crack sealed just by the contribution  
574 of autogenous healing in the REF series. This partial closure and the opposite results if  
575 considering the good behavior showed by the BAC series during the water flow test, could  
576 be partially attributed to the drying procedure, that could have caused the shrinkage of the  
577 silica gel and partial detachment from the crack faces and internal damage in the sealing  
578 material (see Fig. 15).

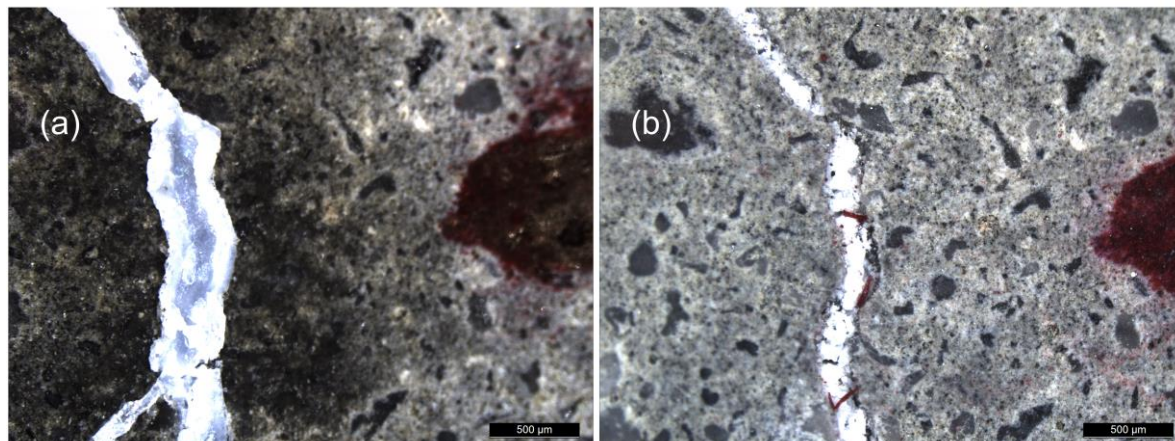


**Fig. 15.** Visualization of one fixed crack mouth location filled with the silica-sol of the BAC series: (a) after crack creation and (b) after the drying process, where it is possible to notice partial detachment and damaged zone that could have caused a partial re-opening of the crack before the water absorption test.

Lastly, it should be noted that the cementitious capsules act in a way similar to the aggregates in concrete, therefore it is reasonable to consider the existence of an interfacial transition zone (ITZ) between the capsules and the surrounding matrix. This zone leads to a local increase in porosity, with microcracking, that may appear at the interface due to shrinkage or mechanical loading [79,80]. Therefore, microcracking can be expected for the BAC series in contrast to the REF series, also due to the mechanical action exerted by the capsule breakage. For the sake of completeness, it should be noted also that in the case of the BAC series the silica gel immobilized bacteria were not spread extensively on the area adjacent to the crack mouth, similarly to the PUR series, while the deposition medium was spread on the adjacent area, similarly to the WRA series.

Table 5 summarizes the results of the water absorption test, showing the best recovery for the series that used the WRA as healing agent ( $SE_{wa}=92\%$ ), regardless the coating of the capsules. It has to be noted that the sealing efficiency was calculated just as a reduction in terms of sorptivity with respect to a cracked plain mortar matrix, without taking in consideration uncracked reference specimens in order to neutralize the intrinsic matrix sorptivity. It has to be expected that, taking it into account, the behavior of the WRA series would be even better than that of the pristine mortar specimens in terms of absorption properties.

602 **Table 5.** Overview of average sorptivity index  $S$ , standard deviation  $\sigma_s$  and average sealing efficiency  $SE_{wa}$  of  
 603 each series after the water absorption test.

Series	Coating	$S$ (mm/s <sup>0.25</sup> )	$\sigma_s$ (mm/s <sup>0.25</sup> )	$SE_{wa}$ (-)
REF	-	0.26	0.07	-
WRA	INT	0.02	0.01	92%
	EXT	0.02	0.00	92%
PUR	INT	0.15	0.04	41%
	EXT	0.20	0.03	20%
BAC	INT	0.46	0.06	-81%
	EXT	0.63	0.22	-145%

604

## 605 5. Conclusions

606 In this paper, extruded cementitious capsules with two different coating configurations  
 607 were used to encapsulate different healing agents, with the aim of achieving a self-sealing  
 608 system that can increase the durability of newly constructed concrete structures. The used  
 609 healing agents were chosen from the main types commonly used for self-sealing  
 610 applications, namely a water-repellent agent, a polyurethane precursor and a solution of  
 611 silica gel immobilized bacteria.

612 The cementitious capsules were successfully able to sequester and release the healing  
 613 agents with both coating configurations, showing no substantial differences in the  
 614 performance of the healing system for a given healing agent. In fact, the findings obtained  
 615 throughout the investigation were not significantly affected by the different configurations  
 616 of the position of the epoxy coating layer (i.e. applied to the internal or external surface of  
 617 the tubular capsule). The reason for that should rely on the cementitious shell preparation  
 618 and coating procedure. In fact, the primer applied both to the internal and the external  
 619 surfaces of the tubes was sufficient to isolate the healing agents from contact with the  
 620 hardened capsule shell, and hence with the low residual humidity that might be present in it.  
 621 The primary function of the epoxy coating was to offer protection solely against the high  
 622 humidity and high alkalinity of the fresh mortar mix, which represents a major treat for the  
 623 healing agents retention. Therefore, applying it either to the internal or the external surfaces  
 624 of the tubes did not change significantly its performance and allowed to provide a good  
 625 barrier between the healing agents and the harsh environment of the matrix.

626 The active crack width control technique was proven to be effective in reducing the  
 627 variability of the crack induced during the pre-cracking procedure, an aspect of paramount  
 628 importance to improve repeatability of the results and to allow comparison between  
 629 different self-sealing systems, especially when analyzing durability-related properties.

630 As regards the sealing efficiency evaluated with water permeability and water  
 631 absorption, good results were obtained in both tests using the polyurethane precursor (PUR

632 series). When water-repellent agent (WRA series) was used, excellent results were obtained  
633 in preventing the water absorption, while detrimental effects were shown against water  
634 permeability. On the contrary, silica gel immobilized *B. Sphaericus* (BAC series) showed  
635 the inverse behavior, with good results against water permeability and bad results during  
636 water absorption. It can be assumed from these results that, while the PU precursor is well  
637 suited in mitigating both mechanisms, the WRA is well suited when the self-sealing  
638 structure will mainly be exposed to the ingress of deleterious substances governed by  
639 capillary forces, but not when the pressure is the driving force. On the other end, the  
640 bacterial healing agent seems more suited when the water leakage, also in pressure, could  
641 be the cause of the ingress of deleterious substances and losses of serviceability. In light of  
642 these considerations, it can be concluded that the self-sealing systems should be tailor-made  
643 for the real operating conditions that the structure will meet during its service life, by  
644 choosing the correct healing agent, the correct location for the self-sealing system and by  
645 taking advantage of the synergy between different self-sealing mechanisms.

## 646 **Acknowledgements**

647 This work was supported by a STSM Grant (no. 37401) from the COST Action  
648 CA15202 (<http://www.sarcos.eng.cam.ac.uk>). T. Van Mullem acknowledges the support of  
649 the grant (19SCIP-B103706-05) from the Construction Technology Research Program  
650 funded by the Ministry of Land, Infrastructure and Transport of the Korean government. X.  
651 Zhu acknowledges support from the China Scholarship Council (File No. 201706140108)  
652 and BOF co-funding from Ghent University (reference code: 01SC4918). J. Wang has  
653 contributed to this research as postdoctoral fellow of the Research Foundation Flanders  
654 (FWO). The technical support from the staff of the Magnel Laboratory of Concrete  
655 Research is gratefully acknowledged. Buzzi Unicem, API S.p.A. and TRADECC are  
656 thanked for their generous donation of materials.

## 657 **Conflict of Interest Statement**

658 None.

## 659 **References**

- 660 [1] P.J.M. Monteiro, S.A. Miller, A. Horvath, Towards sustainable concrete, *Nat. Mater.* 16 (2017) 698–699.  
661 doi:10.1038/nmat4930.
- 662 [2] I. Vázquez-Rowe, K. Ziegler-Rodriguez, J. Laso, I. Quispe, R. Aldaco, R. Kahhat, Production of cement in Peru:  
663 Understanding carbon-related environmental impacts and their policy implications, *Resour. Conserv. Recycl.* 142 (2018) 283–  
664 292. doi:10.1016/j.resconrec.2018.12.017.
- 665 [3] B. Lothenbach, K. Scrivener, R.D. Hooton, Supplementary cementitious materials, *Cem. Concr. Res.* 41 (2011) 1244–1256.

doi:10.1016/j.cemconres.2010.12.001.

- [4] E. Özbay, M. Erdemir, H.İ. Durmuş, Utilization and efficiency of ground granulated blast furnace slag on concrete properties – A review, *Constr. Build. Mater.* 105 (2016) 423–434. doi:10.1016/J.CONBUILDMAT.2015.12.153.
- [5] N. Alderete, Y. Villagrán, A. Mignon, D. Snoeck, N. De Belie, Pore structure description of mortars containing ground granulated blast-furnace slag by mercury intrusion porosimetry and dynamic vapour sorption, *Constr. Build. Mater.* 145 (2017) 157–165. doi:10.1016/j.conbuildmat.2017.03.245.
- [6] P. Palmero, A. Formia, J.-M. Tulliani, P. Antonaci, Valorisation of alumino-silicate stone muds: From wastes to source materials for innovative alkali-activated materials, *Cem. Concr. Compos.* 83 (2017) 251–262. doi:10.1016/j.cemconcomp.2017.07.011.
- [7] M. Sánchez, P. Faria, L. Ferrara, E. Horszczaruk, H.M. Jonkers, A. Kwiecień, J. Mosa, A. Peled, A.S. Pereira, D. Snoeck, M. Stefanidou, T. Stryzewska, B. Zając, External treatments for the preventive repair of existing constructions: A review, *Constr. Build. Mater.* 193 (2018) 435–452. doi:10.1016/j.conbuildmat.2018.10.173.
- [8] K. van Breugel, Is there a market for self-healing cement-based materials?, in: A.J.M. Schmets, S. van der Zwaag (Eds.), *Proc. First Int. Conf. Self Heal. Mater.*, Springer, Noordwijk aan Zee, the Netherlands, 2007: pp. 1–9.
- [9] N. De Belie, E. Gruyaert, A. Al-Tabbaa, P. Antonaci, C. Baera, D. Bajare, A. Darquennes, R. Davies, L. Ferrara, T. Jefferson, C. Litina, B. Miljevic, A. Otlewska, J. Ranogajec, M. Roig-Flores, K. Paine, P. Lukowski, P. Serna, J.-M. Tulliani, S. Vucetic, J. Wang, H.M. Jonkers, A Review of Self-Healing Concrete for Damage Management of Structures, *Adv. Mater. Interfaces.* 5 (2018) 1800074. doi:10.1002/admi.201800074.
- [10] K. Van Tittelboom, N. De Belie, Self-healing in cementitious materials-a review, *Materials (Basel).* 6 (2013) 2182–2217. doi:10.3390/ma6062182.
- [11] M. de Rooij, K. Van Tittelboom, N. De Belie, E. Schlangen, eds., *Self-healing phenomena in cement-based materials : State-of-the-Art Report of RILEM Technical Committee 221-SHC: Self-Healing Phenomena in Cement-Based Materials*, Springer, 2013.
- [12] L. Ferrara, T. Van Mullem, M.C. Alonso, P. Antonaci, R.P. Borg, E. Cuenca, A. Jefferson, P.-L. Ng, A. Peled, M. Roig-Flores, M. Sanchez, C. Schroefl, P. Serna, D. Snoeck, J.M. Tulliani, N. De Belie, Experimental characterization of the self-healing capacity of cement based materials and its effects on the material performance: A state of the art report by COST Action SARCOS WG2, *Constr. Build. Mater.* 167 (2018) 115–142. doi:10.1016/J.CONBUILDMAT.2018.01.143.
- [13] K. Van Tittelboom, E. Gruyaert, H. Rahier, N. De Belie, Influence of mix composition on the extent of autogenous crack healing by continued hydration or calcium carbonate formation, *Constr. Build. Mater.* 37 (2012) 349–359. doi:10.1016/J.CONBUILDMAT.2012.07.026.
- [14] T.S. Qureshi, A. Al-Tabbaa, Self-healing of drying shrinkage cracks in cement-based materials incorporating reactive MgO, *Smart Mater. Struct.* 25 (2016) 084004. doi:10.1088/0964-1726/25/8/084004.
- [15] T. Qureshi, A. Kanellopoulos, A. Al-Tabbaa, Autogenous self-healing of cement with expansive minerals-I: Impact in early age crack healing, *Constr. Build. Mater.* 192 (2018) 768–784. doi:10.1016/J.CONBUILDMAT.2018.10.143.
- [16] T. Qureshi, A. Kanellopoulos, A. Al-Tabbaa, Autogenous self-healing of cement with expansive minerals-II: Impact of age and the role of optimised expansive minerals in healing performance, *Constr. Build. Mater.* 194 (2019) 266–275. doi:10.1016/J.CONBUILDMAT.2018.11.027.
- [17] K. Sisomphon, O. Copuroglu, E.A.B. Koenders, Effect of exposure conditions on self healing behavior of strain hardening cementitious composites incorporating various cementitious materials, *Constr. Build. Mater.* 42 (2013) 217–224. doi:10.1016/J.CONBUILDMAT.2013.01.012.
- [18] M. Roig-Flores, S. Moscato, P. Serna, L. Ferrara, Self-healing capability of concrete with crystalline admixtures in different environments, *Constr. Build. Mater.* 86 (2015) 1–11. doi:10.1016/j.conbuildmat.2015.03.091.
- [19] L. Ferrara, V. Krelani, M. Carsana, A “fracture testing” based approach to assess crack healing of concrete with and without crystalline admixtures, *Constr. Build. Mater.* 68 (2014) 535–551. doi:10.1016/J.CONBUILDMAT.2014.07.008.
- [20] M. Roig-Flores, F. Pirritano, P. Serna, L. Ferrara, Effect of crystalline admixtures on the self-healing capability of early-age concrete studied by means of permeability and crack closing tests, *Constr. Build. Mater.* 114 (2016) 447–457.

- 712 doi:10.1016/j.conbuildmat.2016.03.196.
- 713 [21] E. Cuenca, A. Tejedor, L. Ferrara, A methodology to assess crack-sealing effectiveness of crystalline admixtures under  
714 repeated cracking-healing cycles, *Constr. Build. Mater.* 179 (2018) 619–632. doi:10.1016/j.conbuildmat.2018.05.261.
- 715 [22] D. Snoeck, S. Steuperaert, K. Van Tittelboom, P. Dubruel, N. De Belie, Visualization of water penetration in cementitious  
716 materials with superabsorbent polymers by means of neutron radiography, *Cem. Concr. Res.* 42 (2012) 1113–1121.  
717 doi:10.1016/J.CEMCONRES.2012.05.005.
- 718 [23] A. Mignon, D. Snoeck, K. D’Halluin, L. Balcaen, F. Vanhaecke, P. Dubruel, S. Van Vlierberghe, N. De Belie, Alginate  
719 biopolymers: Counteracting the impact of superabsorbent polymers on mortar strength, *Constr. Build. Mater.* 110 (2016) 169–  
720 174. doi:10.1016/J.CONBUILDMAT.2016.02.033.
- 721 [24] E. Gruyaert, B. Debbaud, D. Snoeck, P. Díaz, A. Arizo, E. Tziviloglou, E. Schlangen, N. De Belie, Self-healing mortar with pH-  
722 sensitive superabsorbent polymers: testing of the sealing efficiency by water flow tests, *Smart Mater. Struct.* 25 (2016) 084007.  
723 doi:10.1088/0964-1726/25/8/084007.
- 724 [25] A. Mignon, D. Snoeck, P. Dubruel, S. Van Vlierberghe, N. De Belie, A. Mignon, D. Snoeck, P. Dubruel, S. Van Vlierberghe,  
725 N. De Belie, Crack Mitigation in Concrete: Superabsorbent Polymers as Key to Success?, *Materials (Basel)*. 10 (2017) 237.  
726 doi:10.3390/ma10030237.
- 727 [26] D. Snoeck, T. De Schryver, N. De Belie, Enhanced impact energy absorption in self-healing strain-hardening cementitious  
728 materials with superabsorbent polymers, *Constr. Build. Mater.* 191 (2018) 13–22.  
729 doi:10.1016/J.CONBUILDMAT.2018.10.015.
- 730 [27] C. Romero Rodríguez, S. Chaves Figueiredo, M. Deprez, D. Snoeck, E. Schlangen, B. Šavija, Numerical investigation of crack  
731 self-sealing in cement-based composites with superabsorbent polymers, *Cem. Concr. Compos.* 104 (2019) 103395.  
732 doi:10.1016/j.cemconcomp.2019.103395.
- 733 [28] L. Souza, A. Al-Tabbaa, Microfluidic fabrication of microcapsules tailored for self-healing in cementitious materials, *Constr.*  
734 *Build. Mater.* 184 (2018) 713–722. doi:10.1016/J.CONBUILDMAT.2018.07.005.
- 735 [29] A. Kanellopoulos, P. Giannaros, A. Al-Tabbaa, The effect of varying volume fraction of microcapsules on fresh, mechanical  
736 and self-healing properties of mortars, *Constr. Build. Mater.* 122 (2016) 577–593.  
737 doi:10.1016/J.CONBUILDMAT.2016.06.119.
- 738 [30] W. Du, J. Yu, Y. Gu, Y. Li, X. Han, Q. Liu, Preparation and application of microcapsules containing toluene-di-isocyanate for  
739 self-healing of concrete, *Constr. Build. Mater.* 202 (2019) 762–769. doi:10.1016/J.CONBUILDMAT.2019.01.007.
- 740 [31] C. Dry, W. McMillan, Three-part methylmethacrylate adhesive system as an internal delivery system for smart responsive  
741 concrete, *Smart Mater. Struct.* 5 (1996) 297–300. doi:10.1088/0964-1726/5/3/007.
- 742 [32] K. Van Tittelboom, N. De Belie, D. Van Loo, P. Jacobs, Self-healing efficiency of cementitious materials containing tubular  
743 capsules filled with healing agent, *Cem. Concr. Compos.* 33 (2011) 497–505. doi:10.1016/J.CEMCONCOMP.2011.01.004.
- 744 [33] B. Hilloulin, K. Van Tittelboom, E. Gruyaert, N. De Belie, A. Loukili, Design of polymeric capsules for self-healing concrete,  
745 *Cem. Concr. Compos.* 55 (2015) 298–307. doi:10.1016/J.CEMCONCOMP.2014.09.022.
- 746 [34] M. Araújo, S. Chatrabhuti, S. Gurdebeke, N. Alderete, K. Van Tittelboom, J.-M. Raquez, V. Cnudde, S. Van Vlierberghe, N.  
747 De Belie, E. Gruyaert, Poly(methyl methacrylate) capsules as an alternative to the proof-of-concept” glass capsules used in  
748 self-healing concrete, *Cem. Concr. Compos.* 89 (2018) 260–271. doi:10.1016/J.CEMCONCOMP.2018.02.015.
- 749 [35] A. Kanellopoulos, T.S. Qureshi, A. Al-Tabbaa, Glass encapsulated minerals for self-healing in cement based composites,  
750 *Constr. Build. Mater.* 98 (2015) 780–791. doi:10.1016/J.CONBUILDMAT.2015.08.127.
- 751 [36] J. Feiteira, E. Gruyaert, N. De Belie, Self-healing of moving cracks in concrete by means of encapsulated polymer precursors,  
752 *Constr. Build. Mater.* 102 (2016) 671–678. doi:10.1016/J.CONBUILDMAT.2015.10.192.
- 753 [37] P. Van den Heede, B. Van Belleghem, N. Alderete, K. Van Tittelboom, N. De Belie, Neutron Radiography Based Visualization  
754 and Profiling of Water Uptake in (Un)cracked and Autonomously Healed Cementitious Materials., *Materials (Basel)*. 9 (2016).  
755 doi:10.3390/ma9050311.
- 756 [38] J. Wang, K. Van Tittelboom, N. De Belie, W. Verstraete, Use of silica gel or polyurethane immobilized bacteria for self-  
757 healing concrete, *Constr. Build. Mater.* 26 (2012) 532–540. doi:10.1016/j.conbuildmat.2011.06.054.

- 758 [39] H. Mihashi, Y. Kaneko, T. Nishiwaki, K. Otsuka, Fundamental Study on Development of Intelligent Concrete Characterized by  
759 Self-Healing Capability for Strength, *Concr. Res. Technol.* 11 (2000) 21–28. doi:10.3151/crt1990.11.2\_21.
- 760 [40] T. Nishiwaki, H. Mihashi, B.-K. Jang, K. Miura, Development of Self-Healing System for Concrete with Selective Heating  
761 around Crack, *J. Adv. Concr. Technol.* 4 (2006) 267–275. doi:10.3151/jact.4.267.
- 762 [41] C. Joseph, A.D. Jefferson, B. Isaacs, R. Lark, D. Gardner, Experimental investigation of adhesive-based self-healing of  
763 cementitious materials, *Mag. Concr. Res.* 62 (2010) 831–843. doi:10.1680/mac.2010.62.11.831.
- 764 [42] H. Huang, G. Ye, Z. Shui, Feasibility of self-healing in cementitious materials – By using capsules or a vascular system?,  
765 *Constr. Build. Mater.* 63 (2014) 108–118. doi:10.1016/j.conbuildmat.2014.04.028.
- 766 [43] P. Minnebo, G. Thierens, G. De Valck, K. Van Tittelboom, N. De Belie, D. Van Hemelrijck, E. Tsangouri, P. Minnebo, G.  
767 Thierens, G. De Valck, K. Van Tittelboom, N. De Belie, D. Van Hemelrijck, E. Tsangouri, A Novel Design of Autonomously  
768 Healed Concrete: Towards a Vascular Healing Network, *Materials (Basel)*. 10 (2017) 49. doi:10.3390/ma10010049.
- 769 [44] M. Araújo, S. Van Vlierberghe, J. Feiteira, G.J. Graulus, K. Van Tittelboom, J.C. Martins, P. Dubruel, N. De Belie, Cross-  
770 linkable polyethers as healing/sealing agents for self-healing of cementitious materials, *Mater. Des.* 98 (2016) 215–222.  
771 doi:10.1016/j.matdes.2016.03.005.
- 772 [45] M. Araújo, K. Van Tittelboom, P. Dubruel, S. Van Vlierberghe, N. De Belie, Acrylate-endcapped polymer precursors: effect of  
773 chemical composition on the healing efficiency of active concrete cracks, *Smart Mater. Struct.* 26 (2017) 055031.  
774 doi:10.1088/1361-665X/AA64CB.
- 775 [46] P. van den Heede, B. van Belleghem, M.A. Araújo, J. Feiteira, N. de Belie, Screening of Different Encapsulated Polymer-  
776 Based Healing Agents for Chloride Exposed Self-Healing Concrete Using Chloride Migration Tests, *Key Eng. Mater.* 761  
777 (2018) 152–158. doi:10.4028/www.scientific.net/KEM.761.152.
- 778 [47] M. Araújo, N. De Belie, S. Van Vlierberghe, Towards encapsulation of thiol-ene mixtures: Synthesis of thioacetate cross-linker  
779 for in-situ deprotection, *Mater. Lett.* 249 (2019) 165–168. doi:10.1016/j.matlet.2019.04.079.
- 780 [48] H. Huang, G. Ye, Application of sodium silicate solution as self-healing agent in cementitious materials, in: C. Leung, K.T.  
781 Wan (Eds.), *Int. RILEM Conf. Adv. Constr. Mater. Through Sci. Eng.*, RILEM Publications SARL, Hong Kong, China, 2011:  
782 pp. 530–536.
- 783 [49] M. Ait Ouarabi, P. Antonaci, F. Boubenider, A. Gliozzi, M. Scalerandi, Ultrasonic Monitoring of the Interaction between  
784 Cement Matrix and Alkaline Silicate Solution in Self-Healing Systems, *Materials (Basel)*. 10 (2017) 46.  
785 doi:10.3390/ma10010046.
- 786 [50] G. Anglani, P. Antonaci, A.S. Gliozzi, M. Scalerandi, Ultrasonic investigation on the fracture-healing mechanism due to  
787 alkaline silicate solutions, in: E.E. Gdoutos (Ed.), *ICF 2017 - 14th Int. Conf. Fract.*, International Conference on Fracture,  
788 Rhodes, Greece, 2017: pp. 120–121.
- 789 [51] A.S. Gliozzi, M. Scalerandi, G. Anglani, P. Antonaci, L. Salini, Correlation of elastic and mechanical properties of consolidated  
790 granular media during microstructure evolution induced by damage and repair, *Phys. Rev. Mater.* 2 (2018) 013601.  
791 doi:10.1103/PhysRevMaterials.2.013601.
- 792 [52] H.M. Jonkers, A. Thijssen, G. Muyzer, O. Copuroglu, E. Schlangen, Application of bacteria as self-healing agent for the  
793 development of sustainable concrete, *Ecol. Eng.* 36 (2010) 230–235. doi:10.1016/j.ecoleng.2008.12.036.
- 794 [53] J. Wang, Y.C. Ersan, N. Boon, N. De Belie, Application of microorganisms in concrete: a promising sustainable strategy to  
795 improve concrete durability, *Appl. Microbiol. Biotechnol.* 100 (2016) 2993–3007. doi:10.1007/s00253-016-7370-6.
- 796 [54] T.K. Sharma, M. Alazhari, A. Heath, K. Paine, R.M. Cooper, Alkaliphilic *Bacillus* species show potential application in  
797 concrete crack repair by virtue of rapid spore production and germination then extracellular calcite formation, *J. Appl.*  
798 *Microbiol.* 122 (2017) 1233–1244. doi:10.1111/jam.13421.
- 799 [55] K. Van Tittelboom, N. De Belie, F. Lehmann, C.U. Grosse, Acoustic emission analysis for the quantification of autonomous  
800 crack healing in concrete, *Constr. Build. Mater.* 28 (2012) 333–341. doi:10.1016/J.CONBUILDMAT.2011.08.079.
- 801 [56] M. Maes, K. Van Tittelboom, N. De Belie, The efficiency of self-healing cementitious materials by means of encapsulated  
802 polyurethane in chloride containing environments, *Constr. Build. Mater.* 71 (2014) 528–537.  
803 doi:10.1016/J.CONBUILDMAT.2014.08.053.

- 804 [57] K. Van Tittelboom, J. Wang, M. Araújo, D. Snoeck, E. Gruyaert, B. Debbaut, H. Derluyn, V. Cnudde, E. Tsangouri, D. Van  
805 Hemelrijck, N. De Belie, Comparison of different approaches for self-healing concrete in a large-scale lab test, *Constr. Build.*  
806 *Mater.* 107 (2016) 125–137. doi:10.1016/J.CONBUILDMAT.2015.12.186.
- 807 [58] T.S. Qureshi, A. Kanellopoulos, A. Al-Tabbaa, Encapsulation of expansive powder minerals within a concentric glass capsule  
808 system for self-healing concrete, *Constr. Build. Mater.* 121 (2016) 629–643. doi:10.1016/J.CONBUILDMAT.2016.06.030.
- 809 [59] B. Van Belleghem, P. Van den Heede, K. Van Tittelboom, N. De Belie, Quantification of the Service Life Extension and  
810 Environmental Benefit of Chloride Exposed Self-Healing Concrete, *Materials (Basel)*. 10 (2016) 5. doi:10.3390/ma10010005.
- 811 [60] K. Van Tittelboom, E. Tsangouri, D. Van Hemelrijck, N. De Belie, The efficiency of self-healing concrete using alternative  
812 manufacturing procedures and more realistic crack patterns, *Cem. Concr. Compos.* 57 (2015) 142–152.  
813 doi:10.1016/j.cemconcomp.2014.12.002.
- 814 [61] E. Gruyaert, K. Van Tittelboom, J. Sucaet, J. Anrijs, S. Van Vlierberghe, P. Dubruel, B.G. De Geest, J.P. Remon, N. De Belie,  
815 Capsules with evolving brittleness to resist the preparation of self-healing concrete, *Mater. Constr.* 66 (2016) e092.  
816 doi:10.3989/mc.2016.07115.
- 817 [62] J. Feiteira, Self-Healing Concrete Encapsulated Polymer Precursors as Healing Agents for Active Cracks, PhD Thesis, Ghent  
818 University, 2017.
- 819 [63] A. Formia, S. Terranova, P. Antonaci, N.M. Pugno, J.M. Tulliani, Setup of extruded cementitious hollow tubes as  
820 containing/releasing devices in self-healing systems, *Materials (Basel)*. 8 (2015) 1897–1923. doi:10.3390/ma8041897.
- 821 [64] A. Formia, S. Irico, F. Bertola, F. Canonico, P. Antonaci, N.M. Pugno, J.-M. Tulliani, Experimental analysis of self-healing  
822 cement-based materials incorporating extruded cementitious hollow tubes, *J. Intell. Mater. Syst. Struct.* (2016) 1–20.  
823 doi:10.1177/1045389X16635847.
- 824 [65] G. Anglani, P. Antonaci, G. Idone, J.-M. Tulliani, Self-healing of cementitious materials via embedded macro-capsules, in: G.  
825 Ye, Y. Yuan, C. Romero Rodriguez, H. Zhang, B. Šavija (Eds.), *Proc. 4th Int. Conf. Serv. Life Des. Infrastructures*, RILEM  
826 Publications S.A.R.L., Delft, the Netherlands, 2018: pp. 385–388.
- 827 [66] G. Anglani, J.-M. Tulliani, P. Antonaci, Behaviour of Pre-Cracked Self-Healing Cementitious Materials under Static and Cyclic  
828 Loading, *Materials (Basel)*. 13 (2020) 1149. doi:10.3390/MA13051149.
- 829 [67] T. Van Mullem, E. Gruyaert, B. Debbaut, R. Caspeepe, N. De Belie, Novel active crack width control technique to reduce the  
830 variation on water permeability results for self-healing concrete, *Constr. Build. Mater.* 203 (2019) 541–551.  
831 doi:10.1016/j.conbuildmat.2019.01.105.
- 832 [68] B. Mu, Z. Li, S.N.C. Chui, J. Peng, Cementitious composite manufactured by extrusion technique, *Cem. Concr. Res.* 29 (1999)  
833 237–240. doi:10.1016/S0008-8846(98)00097-0.
- 834 [69] H. Lombois-Burger, P. Colombet†, J.L. Halary, H. Van Damme, Kneading and extrusion of dense polymer–cement pastes,  
835 *Cem. Concr. Res.* 36 (2006) 2086–2097. doi:10.1016/J.CEMCONRES.2006.08.001.
- 836 [70] L.K. Aggarwal, P.C. Thapliyal, S.R. Karade, Properties of polymer-modified mortars using epoxy and acrylic emulsions,  
837 *Constr. Build. Mater.* 21 (2007) 379–383. doi:10.1016/j.conbuildmat.2005.08.007.
- 838 [71] E. Tziviloglou, V. Wiktor, H.M. Jonkers, E. Schlangen, Bacteria-based self-healing concrete to increase liquid tightness of  
839 cracks, *Constr. Build. Mater.* 122 (2016) 118–125. doi:10.1016/J.CONBUILDMAT.2016.06.080.
- 840 [72] Y.A. Villagrán Zaccardi, N.M. Alderete, N. De Belie, Improved model for capillary absorption in cementitious materials:  
841 Progress over the fourth root of time, *Cem. Concr. Res.* 100 (2017) 153–165. doi:10.1016/j.cemconres.2017.07.003.
- 842 [73] K.J. Shin, W. Bae, S.-W. Choi, M.W. Son, K.M. Lee, Parameters influencing water permeability coefficient of cracked  
843 concrete specimens, *Constr. Build. Mater.* 151 (2017) 907–915. doi:10.1016/j.conbuildmat.2017.06.093.
- 844 [74] C. Edvardsen, Water Permeability and Autogenous Healing of Cracks in Concrete, *ACI Mater. J.* 96 (1999) 448–454.  
845 doi:10.14359/645.
- 846 [75] K.R. Lauer, F.O. Slate, Autogenous Healing of Cement Paste, *ACI J. Proc.* 52 (1956) 1083–1098. doi:10.14359/11661.
- 847 [76] E.F. Wagner, Autogenous Healing of Cracks in Cement-Mortar Linings for Gray-Iron and Ductile-Iron Water Pipe, *J. Am.*  
848 *Water Works Assoc.* 66 (1974) 358–360. doi:10.2307/41267080.
- 849 [77] S. Jacobsen, J. Marchand, L. Boisvert, Effect of cracking and healing on chloride transport in OPC concrete, *Cem. Concr. Res.*



- 850 26 (1996) 869–881. doi:10.1016/0008-8846(96)00072-5.
- 851 [78] S. Granger, G. Pijaudier Cabot, A. Loukili, D. Marlot, J.C. Lenain, Monitoring of cracking and healing in an ultra high  
852 performance cementitious material using the time reversal technique, *Cem. Concr. Res.* 39 (2009) 296–302.  
853 doi:10.1016/J.CEMCONRES.2009.01.004.
- 854 [79] J.P. Ollivier, J.C. Maso, B. Bourdette, Interfacial transition zone in concrete, *Adv. Cem. Based Mater.* 2 (1995) 30–38.  
855 doi:10.1016/1065-7355(95)90037-3.
- 856 [80] K.L. Scrivener, A.K. Crumie, P. Laugesen, The Interfacial Transition Zone (ITZ) Between Cement Paste and Aggregate in  
857 Concrete, *Interface Sci.* 12 (2004) 411–421. doi:10.1023/B:INTS.0000042339.92990.4c.  
858